Synthesis, biological evaluation and molecular modelling studies of 4-anilinoquinazoline derivatives as protein kinase inhibitors

ARTICLE *in* BIOORGANIC & MEDICINAL CHEMISTRY · JANUARY 2014

Impact Factor: 2.79 · DOI: 10.1016/j.bmc.2014.01.044 · Source: PubMed

7 AUTHORS, INCLUDING:

Digambar Kumar Waiker
Rajiv Gandhi Proudyogiki Vishwavidyalaya
2 PUBLICATIONS **9** CITATIONS
SEE PROFILE

Chandrabose Karthikeyan
Rajiv Gandhi Proudyogiki Vishwavidyalaya
66 PUBLICATIONS **261** CITATIONS
SEE PROFILE

Vasanthanathan Poongavanam
University of Southern Denmark
26 PUBLICATIONS **282** CITATIONS
SEE PROFILE

Laurent Meijer
ManRos Therapeutics
411 PUBLICATIONS **20,688** CITATIONS
SEE PROFILE

Bioorganic & Medicinal Chemistry 22 (2014) 1909–1915

Contents lists available at ScienceDirect

Bioorganic & Medicinal Chemistry

journal homepage: www.elsevier.com/locate/bmc

Synthesis, biological evaluation and molecular modelling studies of 4-anilinoquinazoline derivatives as protein kinase inhibitors

Digambar Kumar Waiker [a,†], Chandrabose Karthikeyan [a,†], Vasanthanathan Poongavanam [b], Jacob Kongsted [b], Olivier Lozach [c], Laurent Meijer [c,d], Piyush Trivedi [a,*]

[a] School of Pharmaceutical Sciences, Rajiv Gandhi Proudyogiki Vishwavidyalaya, Airport Bypass Road, Gandhi Nagar, Bhopal (MP) 462036, India
[b] Department of Physics, Chemistry and Pharmacy, University of Southern Denmark, Odense M, Denmark
[c] Protein Phosphorylation and Human Disease Group, USR3151, Station Biologique, B.P. 74, 29682 Roscoff cedex, Bretagne, France
[d] ManRos Therapeutics, Centre de Perharidy, 29680 Roscoff, Bretagne, France

ARTICLE INFO

Article history:
Received 17 December 2013
Revised 22 January 2014
Accepted 23 January 2014
Available online 31 January 2014

Keywords:
Anilino quinazolines
Protein kinase inhibitor
CLK1 kinase
Docking studies

ABSTRACT

A series of novel 4-anilinoquinazoline derivatives (**3a**–**3j**) has been synthesized and evaluated as potential inhibitors for protein kinases implicated in Alzheimer's disease. Among all the synthesized compounds, compound **3e** (*N*-(3,4-dimethoxyphenyl)-6,7-dimethoxyquinazolin-4-amine) exhibited the most potent inhibitory activity against CLK1 and GSK-3α/β kinase with IC_{50} values of 1.5 μM and 3 μM, respectively. Docking studies were performed to elucidate the binding mode of the compounds to the active site of CLK1 and GSK-3β. The results of our study suggest that compound **3e** may serve as a valuable template for the design and development of dual inhibitors of CLK1 and GSK-3α/β enzymes with potential therapeutic application in Alzheimer's disease.

1. Introduction

The significant increase in the number of incidence of Alzheimer's disease (AD) especially in developed and developing countries is a matter of serious concern. It is predicted that 35 million people are affected by dementia, mainly AD, worldwide and that it will be tripled by the year 2050.[1] Current treatments for AD provide only modest symptomatic relief and there is currently a great need for 'disease modifying' agents that either slow the course of the disease or fully prevent or delay the disease in susceptible individuals.

Protein phosphorylation is the most common post-translational mechanism used by cells to regulate enzymes and structural proteins. The process is controlled by more than 500 protein kinases and 80 protein phosphatases.[2] Since protein phosphorylation is significant for maintenance and regulation of many cellular and physiological processes, abnormal phosphorylation turns out to be a cause or consequence of numerous human diseases such as cancer, diabetes, inflammation, and neurodegenerative diseases.[3–5] Hence, pharmacological inhibitors of kinases have become a major interest in drug discovery.

In AD, aberrant phosphorylation of *tau*, an alternatively spliced microtubule-binding protein, is believed to contribute to neurodegeneration.[6] Hyperphosphorylation of *tau* leads to loss of normal tau functioning and attenuates the stability of neuronal microtubules.[7,8] In addition, *tau* hyperphosphorylation is also associated with aggregation of the protein into neurofibrillary tangles, contributing to neurofibrillary degeneration, neuronal death, and dementia severity.[8,9] A plethora of evidence recorded in the literature suggests that targeting *tau* phosphorylation through inhibition of protein kinases could represent a valid therapeutic approach to reduce *tau* aggregation and associated neuronal death in AD and other neurodegenerative 'taupathies'.[1,10] CDK5/p25, CK1δ/ε, GSK-3α/β, DYRK1A, and CLK1 are involved in the two key molecular features of AD, production of amyloid-β peptides (extracellular plaques) and hyperphosphorylation of the microtubule-binding protein *tau* (intracellular neurofibrillary tangles).[11–13] Consequently, small molecule inhibitors acting on these kinases could be of great therapeutic value in AD and related taupathies.

The quinazoline scaffold has been extensively studied for their many pharmacological properties,[14] which includes anti-cancer,[15] anti-inflammatory,[16–18] anti-bacterial,[19,20] analgesic,[16,18] anti-viral,[21] anti-tubercular,[22] anti-malarial,[23] anti-hypertensive,[24] anti-obesity,[25] anti-diabetic[26] activities. Importantly, 4-anilinoquinazolines have emerged as a versatile template for inhibition of a diverse range of protein kinases.[27] This pharmacophore is present

* Corresponding author. Tel.: +91 755 2678883; fax: +91 755 2742001.
E-mail address: piyush.trivedi@rgtu.net (P. Trivedi).
† These authors contributed equally to this work.

http://dx.doi.org/10.1016/j.bmc.2014.01.044
0968-0896/

in approximately 80% of all ATP-competitive kinases inhibitors that have received approval for treatment of cancer.[28] The spectacular therapeutic and financial success of 4-anilinoquinazoline based kinase inhibitors prompted us investigate their utility as a lead for development of potent inhibitors of CDK5/p25, CK1δ/ε, GSK-3α/β, DYRK1A, and CLK1 enzymes. With this purview, the present work describes synthesis and evaluation of new diversely substituted 4-anilinoquinazolines for inhibitory potency against a panel of five protein kinases (CDK5/p25, CK1δ/ε, GSK-3α/β, DYRK1A, and CLK1).

2. Results and discussion

2.1. Chemistry

The 6,7-dimethoxy-*N*-phenylquinazolin-4-amines (**3a**–**3j**) were synthesized in excellent yields by the reaction of 4-chloro-6,7-dimethoxy quinazoline with aniline substrates under the conditions illustrated in Scheme 1.[29] The structures of the synthesized compounds were assigned based on their elemental analysis and spectral data. For example ^{1}H NMR of **3b** shows a singlet for the NH proton at δ 11.50 and –OCH_3 protons at δ = 4.05 and 4.09 (3H for each) and the aromatic protons were observed as three singlets at δ = 7.40, 8.86, 8.36 (1H for each singlet) and two doublets at δ = 7.59 and 8.08 (with 1H and 2H) and a triplet at δ = 7.67 (with 1H) respectively. Similarly, IR Spectra of 3b shows characteristic peaks at 3340 (NH stretching), 3250 (C=N stretching), 3075 (Ar C–H stretching), 1637 (Ar –C–C– stretching), 1280 (–O–CH_3 stretch), 1068 (–O– stretching), 784 (–CF3 stretching). The Molecular ion peak (M+H) for compound **3b** was observed at *m*/*z* 282.2 in the mass spectra.

2.2. Biological activity

The synthesized 6,7-dimethoxy-*N*-phenylquinazolin-4-amines (**3a**–**3j**) were tested for their potential inhibitory effect on five different kinases namely CDK5/p25 (CDK5/p25), CK1δ/ε (casein kinase 1), GSK-3α/β (Glycogen Synthase Kinase 3α/β), DYRK1A (dual-specificity, tyrosine phosphorylation regulated kinase) and CLK1 (cdc2-like kinase 1). All compounds were first tested at a final concentration of 10 μM. Compounds showing less than 50% inhibition were considered as inactive (IC_{50} >10 μM). Compounds displaying more than 50% inhibition at 10 μM were next tested over a wide range of concentrations (usually 0.01–10 μM) and IC_{50} values were determined from the dose response curves (Sigma-Plot). The results of the in vitro kinase assay are summarized in Table 1.

The results of kinase inhibitory assays demonstrated that none of the synthesized anilino quinazolines showed any inhibitory activity against CDK5/p25, DYRK1A and CK1δ/ε at the maximum concentration tested (10 μM). The 4-anilinoquinazolines appeared to be most effective towards CLK1 as four compounds (**3a**, **3b**, **3e** and **3h**) showed inhibitory activity on the enzyme. Two among the 10 anilinoquinazolines synthesized (compounds **3e** and **3h**) showed significant inhibitory potency against CLK1 at less than 10 μM concentrations (Fig. 1). It is noteworthy that compound **3e** bearing 3, 4 dimethoxy substitution on the aryl ring of the aniline moiety shows less than 5 μM inhibition towards both CLK1 (IC_{50} = 1.5 μM) and GSK-3α/β (IC_{50} = 3 μM) enzymes. Surprisingly, compound **3h** with 3-fluoro and 4-chloro substitution in the aryl ring exhibited a 5 fold reduced inhibition on CLK1 (IC_{50} = 7.6 μM) and no inhibition on GSK-3α/β.

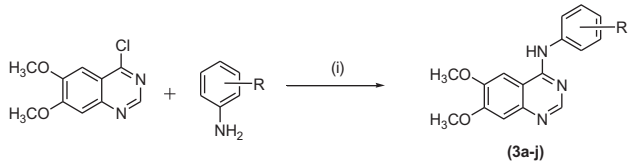

Reagents and conditions: (i) Isopropanol, 90^{0}C, 2-3 hrs

Scheme 1. Synthesis of 6,7-dimethoxy-*N*-phenylquinazolin-4-amines (**3a**–**3j**).

Table 1
Structural data and kinase inhibitory activity of 6,7-dimethoxy-*N*-phenylquinazolin-4-amines

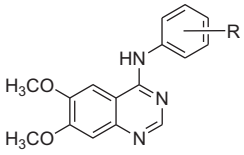

(3a-3j)

Compound	R	IC_{50} (μM)				
		CDK5	CK1	CLK1	DYRK1A rat	GSK-3α/β
3a	H	>10	>10	⩾**10**	>10	>10
3b	3-CF_3	>10	>10	>10	>10	>10
3c	3,4-Dimethyl	>10	>10	>10	>10	>10
3d	4-$COCH_3$	>10	>10	⩾**10**	>10	>10
3e	3,4-Dimethoxy	>10	>10	**1.5**	⩾**10**	**3**
3f	4-OCH_3	>10	>10	>10	>10	>10
3g	4-$NHCOCH_3$	>10	>10	>10	>10	>10
3h	3-Cl, 4-F	>10	>10	**7.6**	>10	>10
3i	4-CF_3	>10	>10	>10	>10	>10
3j	4-OCF_3	>10	>10	>10	>10	>10
6BIO[a]	—	0.083	1.9	2.1	0.52	0.005

[a] Positive control.

2.3. Molecular modeling studies

Molecular modeling studies were performed in order to validate the kinase inhibitory profile shown by 4-anilinoquinazolines and provide better insight into the binding mode of this family of compounds to the CLK1 and GSK-3β kinases. To this end, compounds **3e** and **3h** were docked into the CLK1 and GSK-3β ATP binding site. The crystallographic structures of the CLK1 enzyme in complex with debromohymenialdisine, DBHD, (PDB ID: 1Z57) and GSK-3β in complex with 5-aryl-4-carboxamide-1,3-oxazoles (PDB ID: 4AFJ) were used as protein models for the InducedFit docking (IFD) experiments, which take into account both receptor and ligand flexibility during the docking.

In order to determine whether a docking scheme is applicable to a given system, initially, the crystal structure-based binding pose observed for the bound ligand should be reproduced by re-docking. To this end DBHD was redocked into the receptor with a root-mean-square-deviation of 0.30 Å. In addition to the bound ligand (DBHD), hymenialdisine (HD, a known CLK1 inhibitor and a bromo derivative of DBHD) was also considered in the IFD experiments in order to compare the predicted binding mode with that of the synthesized compounds (e.g., **3e** and **3h**). The active site of human CLK1 has previously been well characterized as being narrow and mainly formed by the backbone of residues PHE172, LYS191, PHE241, GLU242, LEU243, LEU244, ASN293, VAL324 and ASP325. The protein bound water molecules also play a key role in stabilizing the protein–inhibitor complex. First, we investigated the binding mode of hymenialdisine using IFD. It is clear from Figure 2A that the HD binding mode is similar to that of DBHD and that the nitrogen atoms of HD are involved in hydrogen bonding with the active site water molecules and side chains of LEU244, GLU242, ASP325 and LYS191, as reported.[30] It has previously been reported that HD interact through two main-chain hydrogen bonds

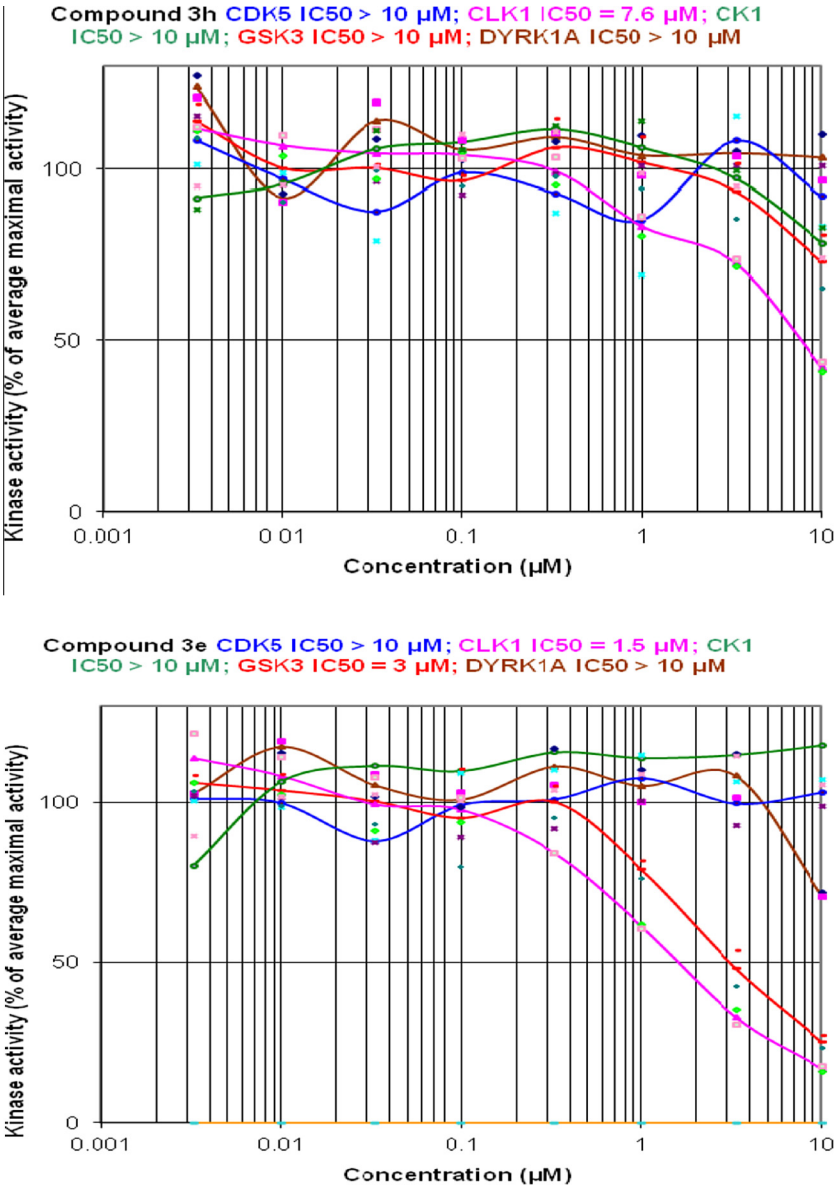

Figure 1. Kinase activity (%) of average max activity for compound **3e** and **3h**.

with the GLU242, LEU243 and LEU244 residues and one hydrogen bond through a water molecule. A similar interaction pattern between the protein–water–ligand was observed from the IFD experiment ($-O_{Ligand}$–LEU244–H_2O–NH_{Ligand}), this observation being in good agreement with the previously reported binding mode of HD and DBH (see the protein–ligand interaction diagram provided in the Supplementary information section).

Compounds **3e** (IC_{50} = 1.5 μM) and **3h** (IC_{50} = 7.5 μM) were shown to be strong inhibitors against human CLK1 in our screening experiments. To investigate a more realistic binding mode of these compounds and how well these compounds are ranked according to the docking fitness function in respect to inhibition, we ran IFD experiments and analyzed the various docking poses. As shown in Figure 2B and C, both compounds bind to the ATP binding site of the kinase through hydrogen bonding and extensive hydrophobic interactions. The quinazoline ring of both compounds **3e** and **3h** is placed above the hinge region of the kinase facilitating hydrogen bonding between the quinazoline nitrogen (N1) and LEU241 which is deemed to be important for inhibitor potency. Compound **3e** exhibited four hydrogen bonds with amino acid residues LEU241, GLU292, ASN 293 in the kinase. The anilino 'NH' group of compound **3e** formed a hydrogen bond with LEU241 and the quinazoline nitrogen (N3) formed a water mediated hydrogen bond with LEU167 of the kinase. The oxygen of the dimethoxy substitution on the anilino phenyl ring also formed hydrogen bonding with the GLU292 and ASN293 residues through a network of water molecules. Overall, compared to **3h**, compound **3e** strongly binds with residues through various hydrogen-bonding network. This observation is also reflected from the IFD scores: **3e** (−12.76), **3h** (−10.7) and HD (−10.92).

Among the synthesized compounds, only **3h** is active against GSK-3α/β with inhibitory potency of 3 μM. To differentiate the activity pattern of compound **3h** and **3e** (active against CLK1 and inactive against GSK-3α/β) in terms of its binding mode in GSK-3β, we performed IFD experiments. From the binding pose analysis (Fig. 3A), as expected, both compounds show different interaction patterns with counter partner although both molecules share the common scaffold. The amino group between two aromatic systems of compound **3h** is strongly interacting with the backbone carbonyl group of VAL135 (distance 2.7 Å) as previously observed for

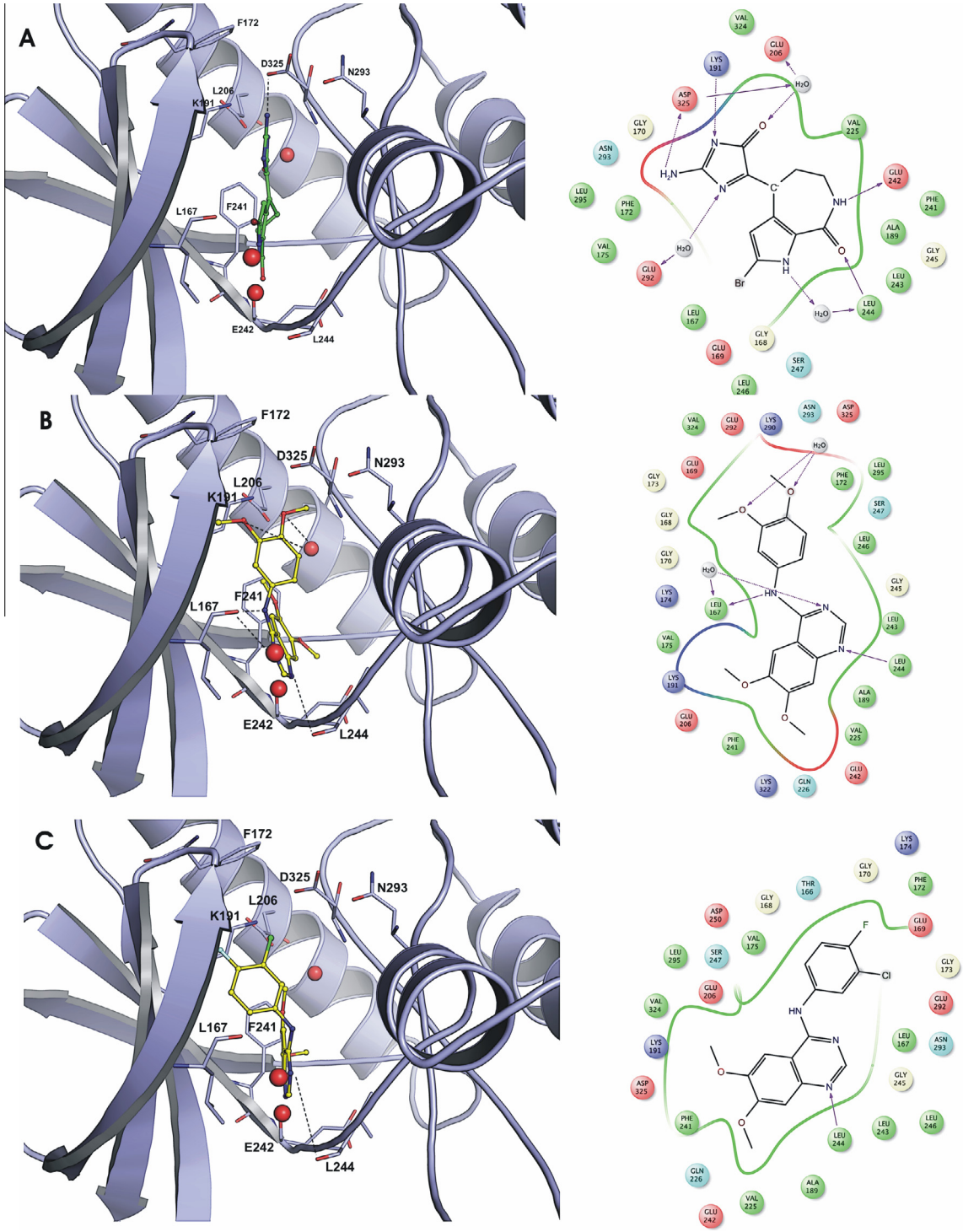

Figure 2. Comparison of the binding mode of bound ligand (A) with the active compounds **3e** (B), **3h** (C) in the CLK1 active site. Important residues are highlighted (cyan stick) including bound waters (red sphere). On the right panel a schematic diagram of the protein–ligand interaction is shown for the bound ligand and the active compounds **3e** and **3h**.

pyridine derivatives for GSK-3β.[31,32] This backbone interaction facilitates a π-cation interaction between ARG141 and the phenyl ring of **3h**, which was not observed for other compounds from this family for example, **3e**. The close proximity (distance 2.8 Å) of the quinazoline ring nitrogen (N3) to amido 'NH' of VAL135 suggests the likelihood of hydrogen bonding interaction between them. Moreover, the 3 methoxy group on the anilino phenyl ring also establishes hydrogen bonding with phenolic hydroxyl group on TYR 134.

On the other hand, the binding pose of **3e** is slightly different compared to **3h**, meaning that the whole molecule is slightly down posed (Fig. 3B). Moreover the NH (4-amino) flipped to the other side of VAL135 (with a distance of 5.7 Å), which may abolish the GSK-3β inhibitory activity. In addition, no significant polar

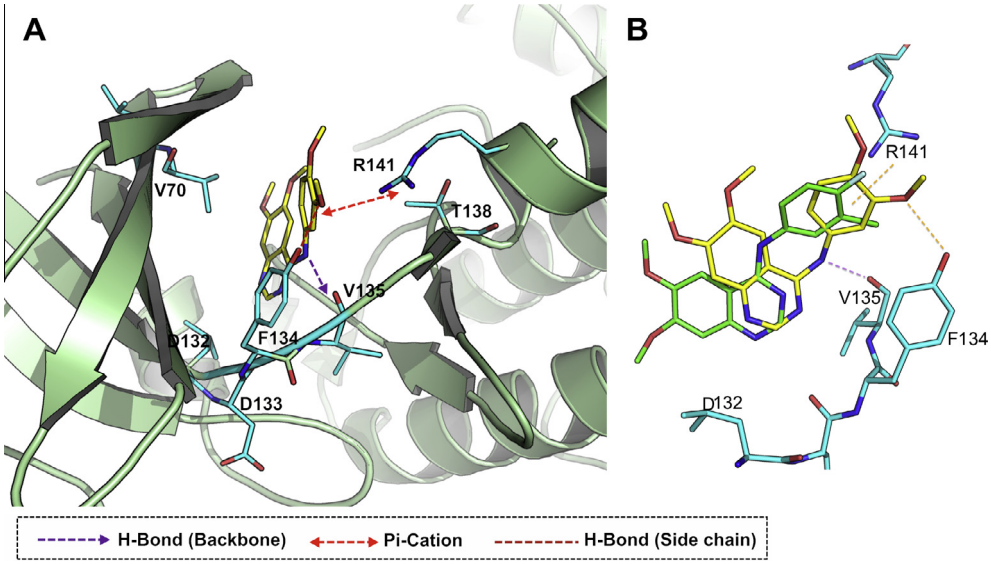

Figure 3. (A) The binding mode of **3e** (yellow) is shown in the GSK3β active site and important residues are highlighted with cyan stick. (B) Comparison of **3e** (yellow) and **3h** (green) binding mode in the active site.

ligand–protein interaction is observed between **3e** and the other active site residues of GSK-3β except for hydrogen bonding between the methoxy group on C6 of the quinazoline ring and LYS85 of the GSK-3β kinase.

3. Conclusion

4-anilinoquinazolines have emerged as a versatile template for inhibitor design for a diverse range of protein kinases. A series of 4-anilinoquinazolines were synthesized and evaluated for their inhibitory activity against five kinases implicated in Alzheimer's and other neurodegenerative diseases. Two compounds namely **3e** and **3h** exhibited good potency for CLK1 kinase in comparison to other structurally related kinases like CDK5/p25, CK1δ/ε and DYRK1A. In addition to potent CLK1 inhibitory activity, compound **3e** also showed potent GSK-3α/β inhibition at less than 5 micromolar concentration, making it particularly promising lead for the development of new dual inhibitors of CLK1 and GSK-3α/β kinases. Docking studies were also performed to understand the binding pattern of the active compounds to the CLK1 and GSK-3α/β kinases. The overall findings of this study exemplify the utility of the 4-anilinoquinazoline scaffold for drug discovery efforts targeted towards kinases related to neurodegenerative diseases. With this understanding, efforts are expended in our laboratory for further optimization of 4-anilinoquinazolines with the hope to develop potent inhibitors of CLK1 and GSK-3α/β kinases with potential therapeutic application in neurodegenerative diseases.

4. Experimental

4.1. Chemistry

All commercial chemicals and solvents used are of reagent grade and were used without further treatment unless otherwise noted. Melting points were determined in open glass capillaries on a Jindal melting point apparatus and were uncorrected. Infrared (IR) spectra were recorded on a Schimadzu FT-IR 8400S infrared spectrophotometer using the ATR accessory. ^{1}H NMR spectra were recorded on a Bruker Avance II 400 spectrometer, using DMSO-d_6 as solvent and TMS as internal standard. Mass spectral analysis was carried out using Applied Biosystem Qtrap 3200 MS/MS system in ESI mode. Reactions were monitored by TLC using precoated silica gel aluminum plates (Kieselgel 60, 254, E. Merck, Germany); zones were detected visually under ultraviolet irradiation.

4.2. General procedure for synthesis of 6,7-dimethoxy-*N*-phenylquinazolin-4-amines (3a–3j)

A mixture of 4-chloro-6,7-dimethoxyquinazoline (1 mmol), aniline (1 mmol) and 2-propanol (5 ml) was refluxed at 90 °C with stirring on oil bath for 2–3 h. Upon completion of the reaction as indicated by a single spot in TLC (Chloroform/Methanol −9:1 as mobile phase), the reaction mixture is cooled to ambient temperature and the solid product precipitated out is filtered. The filtered product is washed with cold 2-propanol and dried.

4.2.1. 6,7-Dimethoxy-*N*-phenylquinazolin-4-amine (3a)

$C_{16}H_{15}N_3O_2$. Yield: 73%, mp 251–253 °C, ^{1}H NMR (DMSO-d_6): δ 4.04 (s, 3H, OCH_3), 4.06 (s, 3H, OCH_3), 7.33 (t, J = 7.40 Hz, 1H, Ar-H), 7.48 (t, J = 8.00 Hz, 2H, Ar-H), 7.67 (d, J = 7.72 Hz, 2H, Ar-H), 8.28 (s, 1H, Ar-H), 8.77 (s, 1H, Ar-H), 11.32 (s, 1H, NH). IR (KBr) ν (cm^{-1}): 3200 (N–H), 3050 (C–H), 1633 (C=N), 1573 (C=C), 1281(C–O), 1232(C–N). MS-API $(M+H)^+$ m/z 282.2 (Calcd 281.12).

4.2.2. 6,7-Dimethoxy-*N*-(3(trifluoromethyl) phenyl)quinazolin-4-amine (3b)

$C_{17}H_{14}F_3N_3O_2$. Yield: 71%, mp 251–253 °C, ^{1}H NMR (DMSO-d_6): δ 4.05 (s, 3H, OCH_3), 4.09 (s, 3H, OCH_3), 7.40 (s, 1H, Ar-H), 7.59 (d, J = 7.88 Hz, 1H, Ar-H) 7.67 (t, J = 7.96 Hz, 1H, Ar-H), 8.08 (d, J = 7.80 Hz, 2H, Ar-H), 8.36 (s, 1H, Ar-H), 8.86 (s, 1H, Ar-H), 11.50 (s, 1H, NH). IR (KBr) ν (cm^{-1}): 3350 (N–H), 3045 (C–H), 1638 (C=N), 1577 (C=C), 1329 (C–N), 1281 (C–O). MS-API $(M+H)^+$ m/z 350.2 (Calcd 349.1).

4.2.3. *N*-(3,4-Dimethylphenyl)-6,7-dimethoxy quinazolin-4-amine (3c)

$C_{18}H_{19}N_3O_2$. Yield: 66%, mp 263–265 °C, ^{1}H NMR (DMSO-d_6): δ 2.55 (s, 3H, CH_3), 4.03 (s, 3H, OCH_3), 4.04 (s, 3H, OCH_3), 7.21 (d, J = 7.80 Hz, 1H, Ar-H), 7.37 (m, 3H, Ar-H), 8.23 (s, 1H, Ar-H), 8.72 (s, 1H, Ar-H), 11.18 (s, 1H, NH). IR (KBr) ν (cm^{-1}): 3200 (N–H), 3050 (C–H), 1633 (C=N), 1573 (C=C), 1286 (C–O), 1229 (C–N), 1121 (C–F). MS-API $(M+H)^+$ m/z 310.2 (Calcd 309.15).

4.2.4. 1-(4-(6,7-Dimethoxyquinazolin-4-yl amino)phenyl) ethanone (3d)

$C_{18}H_{17}N_3O_3$. Yield: 64%; mp 265–267 °C, ^{1}H NMR (DMSO-d_6): δ 2.62 (s, 3H, CH_3), 4.04 (s, 3H, OCH_3), 4.08 (s, 3H, OCH_3), 7.39 (s, 1H, Ar-H), 7.94 (d, J = 8.72 Hz, 2H, Ar-H), 8.05 (d, J = 8.72 Hz, 2H, Ar-H), 8.14 (s, 1H, Ar-H), 8.34 (s, 1H, Ar-H), 11.40 (s, 1H, NH). IR (KBr) ν (cm^{-1}): 3300 (N–H), 3040 (C–H), 1670 (C=O), 1634 (C=N), 1570 (C=C), 1277 (C–O), 1238 (C–N). MS-API $(M+H)^+$ m/z 324.2 (Calculated 323.13).

4.2.5. *N* (3,4 Dimethoxyphenyl) 6,7dimethoxy quinazolin-4-amine (3e)

$C_{18}H_{19}N_3O_4$. Yield: 71%, mp 258–260 °C, ^{1}H NMR (DMSO-d_6): δ 3.85 (s, 3H, OCH_3), 3.87 (s, 3H, OCH_3), 4.04 (s, 6H, OCH_3), 7.01 (d, J = 8.64 Hz, 1H, Ar-H), 7.33 (d, J = 8.60 Hz, 1H, Ar-H), 7.23 (s, 1H, Ar-H), 7.30 (s, 1H, Ar-H), 8.09 (s, 1H, Ar-H), 8.11(s, 1H, Ar-H), 8.74 (s, 1H, Ar-H), 11.12 (s, 1H, NH). IR (KBr) ν (cm^{-1}): 3220 (N–H), 3090 (C–H), 1634 (C=N), 1578 (C=C), 1273 (C–O), 1236 (C–N). MS-API $(M+H)^+$ m/z 342.2 (Calcd 341.14).

4.2.6. 6,7-Dimethoxy-*N*-(4-methoxyphenyl) quinazolin-4-amine (3f)

$C_{17}H_{17}N_3O_3$. Yield: 72%, mp 254–256 °C, ^{1}H NMR (DMSO-d_6): δ 3.83 (s, 3H, OCH_3), 4.02 (s, 3H, OCH_3), 4.05 (s, 3H, OCH_3), 7.0 (d, J = 8.92 Hz, 2H, Ar-H), 7.37 (s, 1H, Ar-H), 7.55 (d, J = 8.88 Hz, 2H, Ar-H), 8.25 (s, 1H, Ar-H), 8.71 (s, 1H, Ar-H), 11.24 (s, 1H, NH). IR (KBr) ν (cm^{-1}): 3391 (N–H), 3030 (C–H), 1632 (C=N), 1514 (C=C), 1280 (C–O), 1245 (C–N). MS-API $(M+H)^+$ m/z 312.0 (Calcd 311.13).

4.2.7. *N*-(4-(6,7-Dimethoxyquinazolin-4-yl amino)phenyl) acetamide (3g)

$C_{18}H_{18}N_4O_3$. Yield: 64%, mp 261–263 °C, ^{1}H NMR (DMSO-d_6): δ 2.11 (s, 3H, OCH_3), 4.36 (s, 3H, OCH_3), 4.05 (s, 3H, OCH_3), 7.37 (s, 1H, Ar-H), 7.56 (d, J = 8.84 Hz, 2H, Ar-H), 7.72 (d, J = 8.88 Hz, 2H, Ar-H), 8.24 (s, 1H, Ar-H), 8.71 (s, 1H, Ar-H), 10.05 (s, 1H, NH), 11.22 (s, 1H, NH). IR (KBr) ν (cm^{-1}): 3208 (N–H), 3100 (C–H), 1680 (C=O), 1641 (C=N), 1516 (C=C), 1277 (C–O), 1234 (C–N). MS-API $(M+H)^+$ m/z 339.2 (Calcd 338.14).

4.2.8. *N*-(3-Chloro-4-fluorophenyl)-6,7-di methoxyquinazolin-4-amine (3h)

$C_{16}H_{13}ClFN_3O_2$. Yield: 82%, mp 273–275 °C, ^{1}H NMR (DMSO-d_6): δ 4.00 (s, 3H, OCH_3), 4.05 (s, 3H, OCH_3), 7.71 (t, J = 4.36 Hz, 1H, Ar-H), 7.40 (t, J = 8.88 Hz, 1H, Ar-H), 7.67 (d, J = 8.4 Hz, 2H, Ar-H), 8.28 (s, 1H, Ar-H), 8.77 (s, 1H, Ar-H), 11.32 (s, 1H, NH). IR (KBr) ν (cm^{-1}): 3200 (N–H), 3036 (C–H), 1638 (C=N), 1578 (C=C), 1283 (C–O) 1227 (C–N), 1157 (C–F), 838 (C–Cl). MS-API $(M+H)^+$ m/z 334 (Calcd 333.07).

4.2.9. 6,7-Dimethoxy-*N*-(4-(trifluoromethyl) phenyl)quinazolin-4-amine (3i)

$C_{17}H_{14}F_3N_3O_2$. Yield: 55%, mp 269–271 °C, ^{1}H NMR (DMSO-d_6): δ 4.01 (s, 3H, OCH_3), 4.05 (s, 3H, OCH_3), 7.39 (s, 1H, Ar-H), 7.73 (d, J = 8.44 Hz, 2H, Ar-H), 7.99 (d, J = 8.36 Hz, 2H, Ar-H), 8.37 (s, 1H, Ar-H), 8.81 (s, 1H, Ar-H), 11.51 (s, 1H, NH). IR (KBr) ν (cm^{-1}): 3300 (N–H), 3032 (C–H), 1635 (C=N), 1572 (C=C), 1234 (C–N), 1282 (C–O), 1234 (C–N), 1072 (C–F). MS-API $(M+H)^+$ m/z 350.0 (Calcd 349.1).

4.2.10. 6,7-Dimethoxy-*N*-(4-(trifluoro methoxy) phenyl) quinazolin-4-amine (3j)

$C_{17}H_{14}F_3N_3O_3$. Yield: 62%, mp 259–261 °C, ^{1}H NMR (DMSO-d_6): δ 4.00 (s, 3H, OCH_3), 4.05 (s, 3H, OCH_3), 7.30 (d, J = 8.56 Hz, 2H, Ar-H), 7.38 (s, 1H, Ar-H), 7.81 (d, J = 8.28 Hz, 2H, Ar-H), 7.94 (s, 1H, Ar-H), 8.35 (s, 1H, Ar-H), 8.70 (s, 1H, Ar-H), 11.64 (s, 1H, NH). MS IR (KBr) ν (cm^{-1}): 3442 (N–H), 3036 (C–H), 1631 (C=N), 1514 (C=C), 1277 (C–N), 1220 (C–O), 1066 (C–F). MS-API $(M+H)^+$ m/z 366.0 (Calcd 365.1).

4.3. Biology

4.3.1. In vitro kinase preparation and assays[33,34]

4.3.1.1. Buffers. *Buffer A:* 10 mM $MgCl_2$, 1 mM ethylene glycol-bis(2-aminoethylether)-*N*,*N*,*N*′,*N*′-tetraacetic acid (EGTA), 1 mM dithio-threitol (DTT), 25 mM Tris–HCl pH 7.5, 50 μg heparin/mL.

Buffer B: 60 mM β-Glycerophosphate, 30 mM *p*-nitro-phenyl-phosphate, 25 mM 3-(*N*-morpholino)propanesulfonic acid (Mops) (pH 7.2), 5 mM EGTA, 15 mM $MgCl_2$, 1 mM DTT, 0.1 mM sodium vanadate.

4.3.1.2. Kinase preparations and assays. Kinase activities were assayed in triplicates in buffer A or B, for 30 min at 30 °C, at a final adenosine triphosphate (ATP) concentration of 15 μM. Blank values were subtracted and activities expressed in % of the maximal activity, that is, in the absence of inhibitors. Controls were performed with appropriate dilutions of dimethylsulfoxide (DMSO). 6 bromoindirubin-3′-monoxime (6BIO), a potent inhibitor of several kinases was used as positive control. IC_{50} values were calculated from dose–response curves established by Sigma-Plots. The GSK-3, CK1, DYRK1A and CLK1 peptide substrates were obtained from Proteogenix (Oberhausbergen, France).

4.3.1.2.1. CDK5/p25. CDK5/p25 (Human, recombinant) was prepared as previously described.[35,36] Its kinase activity was assayed in buffer A, with 1 mg of histone H1/mL, in the presence of 15 μM [γ^{-33} P] ATP (3000 Ci/mmol; 10 mCi/mL) in a final volume of 30 μL. After 30 min incubation at 30 °C, 25 μL aliquots of supernatant were spotted onto sheets of Whatman P81 phosphocellulose paper, and 20 s later, the filters were washed eight times (for at least 5 min each time) in a solution of 10 mL phosphoric acid/L of water. The wet filters were counted in the presence of 1 mL ACS (Amersham) scintillation fluid.

4.3.1.2.2. GSK-3α/β. GSK-3α/β (Porcine brain, native) was assayed, as described for CDK5/p25 but in buffer A and using a GSK-3 specific substrate (GS-1: YRRAAVPPSPSLSRHSSPHQpSEDEEE) (pS stands for phosphorylated serine).[37]

4.3.1.2.3. CK1δ/ε. CK1δ/ε (Porcine brain, native) was assayed as described for CDK5/p25 but using the CK1-specific peptide substrate RRKHAAIGpSAYSITA.[38]

4.3.1.2.4. DYRK1A. DYRK1A (Rat, recombinant, expressed in *Escherichia coli* as a glutathione transferase (GST) fusion protein) was purified by affinity chromatography on glutathione agarose and assayed, as described for CDK5/p25 using Woodtide (KKISGRL-SPIMTEQ) (1.5 μg/assay) as a substrate.

4.3.1.2.5. CLK1. CLK1 (Human, recombinant, expressed in *E. Coli* as GST fusion protein) was assayed in buffer A (+0.15 mg BSA/mL) with RS peptide (GRSRSRSRSRSR) (1 μg/assay).

4.4. Molecular modelling studies

4.4.1. Preparation of protein and ligands

The atomic coordinates of human CLK1 kinase domains in complex with debromo hymenialdisine (PDB ID: 1Z57), as obtained by X-ray crystallography with resolution of 1.7 Å, and atomic coordinates of human GSK-3β kinase in complex with 5-(4-methoxyphenyl)-*N*-(pyridin-4-ylmethyl)-1,3-oxazole-4-carboxamide (PDB ID: 4AFJ) with resolution of 1.98 Å were downloaded from the Protein Data Bank. The structures were imported into the Maestro module (v9.3) available in the Schrödinger package (v2012)[39] and the protein was optimized using the Protein Preparation Wizard.[40] This optimization includes adding hydrogen atoms, assigning correct bond orders and building disulfide bonds. The protonation states of all of the ionizable residues were predicted

by PROPKA (41) provided in the protein preparation wizard. An optimized structure model was energy minimized (only hydrogen atoms) using the OPLS2005 force field. Water molecules in the active site beyond 3 Å from the bound ligand were deleted and optimized as part of the protein.

3D structures of **3e**, **3h** and hymenialdisine (HD) were built with Maestro. Energy minimization was performed using the OPLS-2005 force field and the compounds were pre-processed (e.g., determination of ionization states at pH = 7 (±2) as well as prediction of the most probable tautomers) by the LigPrep module (v2.5) of the Schrödinger modelling software.

4.4.2. Induced fit docking

In order to consider the flexibility of both the protein and ligand in the docking experiments, the Induced Fit Docking (IFD) workflow[41] as implemented in the Schrödinger modelling software was used. A detailed account of the theory behind this method can be found elsewhere.[42,43] The binding site for IFD experiment was defined by the receptor grid generation. For this we defined the grid centered at the bound ligand utilizing the automatic box size option (meaning that the program automatically determine the size of the box according to the size of the bound ligand). During the IFD workflow, the ligands were initially docked into the receptor using the Glide program[42] with the van der Waals radii scaling of 0.5 for the both the ligands and the receptor.

Furthermore, A maximum of 20 top poses for each of the ligands were retained for protein flexibility sampling using the the Prime module[41] of the Schrödinger software. Residues within 5 Å from the ligands in any of the top poses were included for conformation search and energy minimization and the complexes (receptor–ligand conformations) which have energy of <30 kcal/mol were considered for the re-docking step using the extra precision (XP) mode in the Glide program.

Acknowledgments

The authors gratefully acknowledge the Sophisticated Analytical Instrumentation Facility (SAIF); Panjab University, Chandigarh for the NMR spectral analysis of the compounds used in this study. DG wishes to thank AICTE, New Delhi for a postgraduate fellowship. The work was also supported by the EEC FP7-KBBE-2012 BlueGenics grant (LM), 'Institut National contre le Cancer' (INCa) GLIOMER program and the 'Fonds Unique Interministériel' (FUI) PHARMASEA project (LM).

Supplementary data

Supplementary data associated with this article can be found, in the online version, at http://dx.doi.org/10.1016/j.bmc.2014.01.044. These data include MOL files and InChiKeys of the most important compounds described in this article.

References and notes

1. Hanger, D. P.; Anderton, B. H.; Noble, W. *Trends Mol. Med.* **2009**, *15*, 112.
2. Meijer, L.; Flajolet, M.; Greengard, P. *Trends Pharmacol. Sci.* **2004**, *25*, 471.
3. Polychronopoulos, P.; Magiatis, P.; Skaltsounis, A. L.; Myrianthopoulos, V.; Mikros, E.; Tarricone, A.; Musacchio, A.; Roe, S. M.; Pearl, L.; Leost, M.; Greengard, P.; Meijer, L. *J. Med. Chem.* **2004**, *47*, 935.
4. Cohen, P. *Eur. J. Biochem.* **2001**, *268*, 5001.
5. Cohen, P. *Nat. Rev. Drug Disc.* **2002**, *1*, 309.
6. Perl, D. P. *Mt. Sinai J. Med.* **2010**, *77*, 32.
7. Trinczek, B.; Biernat, J.; Baumann, K.; Mandelkow, E. M.; Mandelkow, E. *Mol. Biol. Cell* **1995**, *6*, 1887.
8. Smith, B.; Medda, F.; Gokhale, V.; Dunckley, T.; Hulme, C. *ACS Chem. Neurosci.* **2012**, *3*, 857.
9. Arriagada, P. V.; Growdon, J. H.; Hedley-Whyte, E. T.; Hyman, B. T. *Neurology* **1992**, *42*, 631.
10. Churcher, I. *Curr. Top. Med. Chem.* **2006**, *6*, 579.
11. Martin, L.; Latypova, X.; Wilson, C. M.; Magnaudeix, A.; Perrin, M.-L.; Yardin, C.; Terro, F. *Ageing Res. Rev.* **2013**, *12*, 289.
12. Flight, M. H. *Nat. Rev. Drug Disc.* **2013**, *12*, 739.
13. Hartmann, A. M.; Rujescu, D.; Giannakouros, T.; Nikolakaki, E.; Goedert, M.; Mandelkow, E. M.; Gao, Q. S.; Andreadis, A.; Stamm, S. *Mol. Cell. Neurosci.* **2001**, *18*, 80.
14. Wang, D.; Gao, F. *Chem. Cent. J.* **2013**, *7*, 95.
15. Marzaro, G.; Guiotto, A.; Chilin, A. *Exp. Opin. Ther. Pat.* **2012**, *22*, 223.
16. Alafeefy, A. M.; Kadi, A. A.; Al-Deeb, O. A.; El-Tahir, K. E.; Al-Jaber, N. A. *Eur. J. Med. Chem.* **2010**, *45*, 4947.
17. Gineinah, M. M.; El-Sherbeny, M. A.; Nasr, M. N.; Maarouf, A. R. *Arch. Pharm.* **2002**, *335*, 556.
18. Rather, B. A.; Raj, T.; Reddy, A.; Ishar, M. P.; Sivakumar, S.; Paneerselvam, P. *Arch. Pharm.* **2010**, *343*, 108.
19. Jantova, S.; Greif, G.; Spirkova, K.; Stankovsky, S.; Oravcova, M. *Folia Microbiol.* **2000**, *45*, 133.
20. Parhi, A. K.; Zhang, Y.; Saionz, K. W.; Pradhan, P.; Kaul, M.; Trivedi, K.; Pilch, D. S.; LaVoie, E. J. *Bioorg. Med. Chem. Lett.* **2013**, *23*, 4968.
21. el-Sherbeny, M. A.; Gineinah, M. M.; Nasr, M. N.; el-Shafeih, F. S. *Arzneim.-Forsch.* **2003**, *53*, 206.
22. Kuneš, J.; Bažant, J.; Pour, M.; Waisser, K.; Šlosárek, M.; Janota, J. *Il Farmaco* **2000**, *55*, 725.
23. Verhaeghe, P.; Dumètre, A.; Castera-Ducros, C.; Hutter, S.; Laget, M.; Fersing, C.; Prieri, M.; Yzombard, J.; Sifredi, F.; Rault, S.; Rathelot, P.; Vanelle, P.; Azas, N. *Bioorg. Med. Chem. Lett.* **2011**, *21*, 6003.
24. Tsai, L. M.; Yang, S. N.; Lee, S. F.; Ding, Y. A.; Chern, J. W.; Yang, J. M. *J. Cardiovasc. Pharmacol.* **2001**, *38*, 893.
25. Sasmal, S.; Balasubrahmanyam, D.; KannaReddy, H. R.; Balaji, G.; Srinivas, G.; Cheera, S.; Abbineni, C.; Sasmal, P. K.; Khanna, I.; Sebastian, V. J.; Jadhav, V. P.; Singh, M. P.; Talwar, R.; Suresh, J.; Shashi kumar, D.; Harinder Reddy, K.; Sihorkar, V.; Frimurer, T. M.; Rist, Ø.; Elster, L.; Högberg, T. *Bioorg. Med. Chem. Lett.* **2012**, *22*, 3163.
26. Iino, T.; Sasaki, Y.; Bamba, M.; Mitsuya, M.; Ohno, A.; Kamata, K.; Hosaka, H.; Maruki, H.; Futamura, M.; Yoshimoto, R.; Ohyama, S.; Sasaki, K.; Chiba, M.; Ohtake, N.; Nagata, Y.; Eiki, J.-I.; Nishimura, T. *Bioorg. Med. Chem. Lett.* **2009**, *19*, 5531.
27. Shewchuk, L.; Hassell, A.; Wisely, B.; Rocque, W.; Holmes, W.; Veal, J.; Kuyper, L. F. *J. Med. Chem.* **2000**, *43*, 133.
28. Loidreau, Y.; Marchand, P.; Dubouilh-Benard, C.; Nourrisson, M. R.; Duflos, M.; Lozach, O.; Loaec, N.; Meijer, L.; Besson, T. *Eur. J. Med. Chem.* **2012**, *58*, 171.
29. Ban, H. S.; Tanaka, Y.; Nabeyama, W.; Hatori, M.; Nakamura, H. *Bioorg. Med. Chem.* **2010**, *18*, 870.
30. Bullock, A. N.; Das, S.; Debreczeni, J. É.; Rellos, P.; Fedorov, O.; Niesen, F. H.; Guo, K.; Papagrigoriou, E.; Amos, A. L.; Cho, S.; Turk, B. E.; Ghosh, G.; Knapp, S. *Structure* **2009**, *17*, 352.
31. Chioua, M.; Samadi, A.; Soriano, E.; Lozach, O.; Meijer, L.; Marco-Contelles, J. *Bioorg. Med. Chem. Lett.* **2009**, *19*, 4566.
32. Witherington, J.; Bordas, V.; Garland, S. L.; Hickey, D. M. B.; Ife, R. J.; Liddle, J.; Saunders, M.; Smith, D. G.; Ward, R. W. *Bioorg. Med. Chem. Lett.* **2003**, *13*, 1577.
33. Loidreau, Y.; Marchand, P.; Dubouilh-Benard, C.; Nourrisson, M.-R.; Duflos, M.; Lozach, O.; Loaëc, N.; Meijer, L.; Besson, T. *Eur. J. Med. Chem.* **2012**, *58*, 171.
34. Giraud, F.; Alves, G.; Debiton, E.; Nauton, L.; Théry, V.; Durieu, E.; Ferandin, Y.; Lozach, O.; Meijer, L.; Anizon, F.; Pereira, E.; Moreau, P. *J. Med. Chem.* **2011**, *54*, 4474.
35. Bach, S.; Knockaert, M.; Reinhardt, J.; Lozach, O.; Schmitt, S.; Baratte, B.; Koken, M.; Coburn, S. P.; Tang, L.; Jiang, T.; Liang, D.-C.; Galons, H.; Dierick, J.-F.; Pinna, L. A.; Meggio, F.; Totzke, F.; Schächtele, C.; Lerman, A. S.; Carnero, A.; Wan, Y.; Gray, N.; Meijer, L. *J. Biol. Chem.* **2005**, *280*, 31208.
36. Leclerc, S.; Garnier, M.; Hoessel, R.; Marko, D.; Bibb, J. A.; Snyder, G. L.; Greengard, P.; Biernat, J.; Wu, Y.-Z.; Mandelkow, E.-M.; Eisenbrand, G.; Meijer, L. *J. Biol. Chem.* **2001**, *276*, 251.
37. Primot, A.; Baratte, B.; Gompel, M.; Borgne, A.; Liabeuf, S.; Romette, J.-L.; Jho, E.-H.; Costantini, F.; Meijer, L. *Protein Expr. Purif.* **2000**, *20*, 394.
38. Reinhardt, J.; Ferandin, Y.; Meijer, L. *Protein Expr. Purif.* **2007**, *54*, 101.
39. Schrödinger Suite (2012) Schrödinger, LLC, New York, NY.
40. Madhavi Sastry, G.; Adzhigirey, M.; Day, T.; Annabhimoju, R.; Sherman, W. *J. Comput. Aided Mol. Des.* **2013**, *27*, 221.
41. Li, H.; Robertson, A. D.; Jensen, J. H. *Proteins* **2005**, *61*, 704.
42. Induced Fit Docking protocol; Glide version 5.8, Schrödinger, LLC, New York, NY, 2012; Prime version 3.1, Schrödinger, LLC, New York, NY, 2012.
43. Sherman, W.; Day, T.; Jacobson, M. P.; Friesner, R. A.; Farid, R. *J. Med. Chem.* **2006**, *49*, 534.